

# Defect Solutions of the Non-reciprocal Cahn-Hilliard Model: Spirals and Targets

Navdeep Rana<sup>1</sup> and Ramin Golestanian<sup>1,2</sup>

<sup>1</sup>Max Planck Institute for Dynamics and Self-Organization (MPI-DS), D-37077 Göttingen, Germany

<sup>2</sup>Rudolf Peierls Centre for Theoretical Physics, University of Oxford, Oxford OX1 3PU, United Kingdom

We study the defect solutions of the Non-reciprocal Cahn-Hilliard model (NRCH). We find two kinds of defects, spirals with unit magnitude topological charge, and topologically neutral targets. These defects generate radially outward travelling waves and thus break the parity and time-reversal symmetry. For a given strength of non-reciprocity, spirals and targets with unique asymptotic wavenumber and amplitude are selected. We use large-scale simulations to show that at low non-reciprocity  $\alpha$ , a quenched disordered state evolves into quasi-stationary spiral networks. With increasing  $\alpha$ , we observe networks composed primarily of targets. Beyond a critical threshold  $\alpha_c$ , a disorder-order transition to from defect networks to travelling waves emerges. The transition is marked by a sharp rise in the global polar order.

*Introduction.*—Constituents of active matter, biological or synthetic, interact in complex ways [1]. These interactions are realized through various mechanisms, for example, chemical activity in colloids and enzymes [2, 3], wake-mediated interactions in complex binary plasmas [4], visual perception in bird flocks [5], social communication in crowds of humans [6–8] and microswimmers [9], tensorial hydrodynamic interactions in active carpets [10], and programmable logic in robots [11]. Breaking the action-reaction symmetry leads to novel features that are absent in equilibrium [4, 12], including the possibility to engineer multifarious self-organization of building clocks in a choreographed manner [13]. Individuals in a chemically active mixture can assemble into self-propelling small molecules [2, 14] or form large comet-like clusters [15, 16]. Non-reciprocal alignment interactions lead to a buckling instability of the ordered state in polar flocks [17], as well as a wide range of other novel features [18–20]. In the recently introduced non-reciprocal Cahn-Hilliard model (NRCH) [21–23], parity and time-reversal (PT) symmetries break spontaneously which leads to the formation of travelling density bands [21, 22], coarsening arrest [21, 24], and localized states [25]. A variant of the NRCH model with nonlinear non-reciprocal interactions exhibits chaotic steady states where PT symmetry is restored locally in fluctuating domains [23]. Although the NRCH model was introduced phenomenologically [21, 22], it has been highlighted recently that it is possible to derive it as a universal amplitude equation that emerge from a conserved-Hopf instability, occurring in systems with two conservation laws [26].

In this paper, we study the defect solutions of the NRCH model [21, 22]. We find two types of defects, spirals with a unit magnitude topological charge and topologically neutral targets (see Fig. 1 and Fig. 2). They are the generators of travelling waves and thus break the PT symmetry. In addition, spirals break the chiral symmetry. Spirals are frequently observed and extensively studied in various systems described by the complex Ginzburg-Landau (CGL) equation, for example, the well-known Belousov-Zhabotinskii reaction [27–30], and

colonies of *Dictyostelium* [31]. Topologically neutral targets are unstable in the framework of the CGL equation but can be stabilized by introducing spatial inhomogeneities [30, 32, 33]. In the context of non-reciprocal interactions, creation and annihilation of spiral defects has been reported in the context of active turbulence in wet polar active carpets [10]. Programmable robots are shown to break the chiral symmetry and spontaneously rotate in clockwise or anticlockwise manner [11].

*Summary of results.*—Our central finding is that the NRCH model admits stable spiral and target defect solutions. Remarkably, no additional spatial inhomogeneities are needed to stabilize the targets [32]. For a given strength of non-reciprocal interactions ( $\alpha$ ), defect solutions with a unique asymptotic wave number ( $k_\infty = C\sqrt{\alpha}$ ) and amplitude ( $R_\infty = \sqrt{1 - k_\infty^2}$ ) are selected (see Fig. 2). As a consequence of the wave number selection, defect solutions cease to exist beyond a crossover point  $\alpha_\times = 1/C^2$ . However, in our large-scale numerical simulations of quenched disordered states, defect solutions vanish for  $\alpha$  well below  $\alpha_\times$  and we find a disorder-order transition at  $\alpha_c \ll \alpha_\times$  (see Fig. 1 and Fig. 3). Below  $\alpha_c$ , an initially disordered state evolves

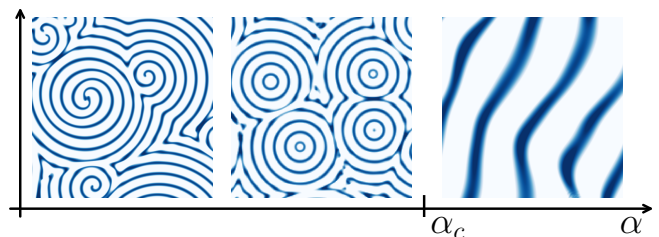


FIG. 1. Qualitative phase portrait for the NRCH model (1) in the  $\alpha$  space. A critical threshold  $\alpha_c$  marks the onset of a disorder-order transition. When non-reciprocal interactions are weak ( $\alpha \ll \alpha_c$ ), we find defect networks with isolated and bound spirals. With increasing  $\alpha$ , targets begin to emerge and are the dominant defects right below  $\alpha_c$ . Above  $\alpha_c$ , noisy global polar order sets in. Fluctuations decay with time which eventually leads to travelling bands.

into quasi-stationary defect network with no global polar order (see Movie 2). While both kinds of defect are stable for a given  $\alpha$ , defect networks exhibit a clear preference for spirals or targets. At small  $\alpha$ , we exclusively find spirals. As we increase  $\alpha$ , targets start to appear as well, and close to the transition point  $\alpha \lesssim \alpha_c$ , we find target-dominated defect networks. Above  $\alpha_c$ , we find travelling waves that show global polar order, rendered imperfect by mesoscopic fluctuations that decay with time and eventually lead to travelling bands. A sharp jump in the global polar order marks the onset of this transition.

*Model.*—We consider a minimal model of two conserved scalar fields  $\phi_1(\mathbf{r}, t)$  and  $\phi_2(\mathbf{r}, t)$  with non-reciprocal interactions. The complex scalar order parameter  $\phi = \phi_1 + i\phi_2$  obeys the following non-dimensional equation [34]

$$\partial_t \phi = \nabla^2 [-(1 + i\alpha)\phi + |\phi|^2\phi - \nabla^2\phi], \quad (1)$$

where the parameter  $\alpha$  measures the strength of the non-reciprocal interactions between  $\phi_1$  and  $\phi_2$ . Conservation of particle numbers for both species makes it impossible to eliminate  $\alpha$  using a global phase transformation as is customarily done for CGL equation [33]. The length scales of interest are the system size  $L$ , the spinodal instability cutoff length  $\ell$  which for (1) is set to unity, and the length scale governing the oscillatory features  $\ell_\alpha = \ell/\sqrt{\alpha}$  [34]. Travelling wave solutions of (1) have the form

$$\phi(\mathbf{r}, t) = R e^{i(\mathbf{k}\cdot\mathbf{r} - \omega t)}, \quad (2)$$

with  $k = |\mathbf{k}|$ ,  $R = \sqrt{1 - k^2}$ , and  $\omega = -\alpha k^2$ . For a given  $\alpha$ , an infinite number of plane waves with  $k < 1$  are possible [33]. These solutions are linearly stable and small perturbations at wave number  $q$  decay with a rate  $\mathcal{O}(q^2)$  [23, 34, 35].

*Defect solutions.*—We now show that the NRCH model (1) admits defect solutions of the form

$$\phi(\mathbf{r}, t) = R(r) e^{i[m\theta - Z(r) - \omega t]}, \quad (3)$$

where  $r$  and  $\theta$  represent the polar coordinates, and  $r$  is measured from the defect core.  $R(r)$  is the amplitude,  $Z(r)$  is the phase, and  $m$  is the topological charge. A target defect does not carry a topological charge ( $m = 0$ ), whereas a spiral has a unit magnitude charge ( $m = \pm 1$ ). Figure 2(a) shows defect solutions for different  $m$ . In Fig. 2(b), we plot  $R(r)$  vs.  $r$  for various values of  $\alpha$  and  $m$ . An isolated spiral core is singular and stationary, thus  $R(r)$  vanishes at the origin and is independent of time. On the other hand, a target is topologically neutral and its amplitude remains finite at the core [27, 32, 33]. The amplitude near the core oscillates slowly for the targets, as in the case of inhomogeneous CGL equation [32]. At small  $r$ ,  $R(r) \sim A(r - r^3/12)$  for spirals and  $R(r) \sim R_0(\alpha) - Br^2$  for targets. For both kinds of defect,  $k(r) \equiv \frac{dZ}{dr} \sim r$  at small  $r$  [34]. Solutions with  $|m| > 1$  are

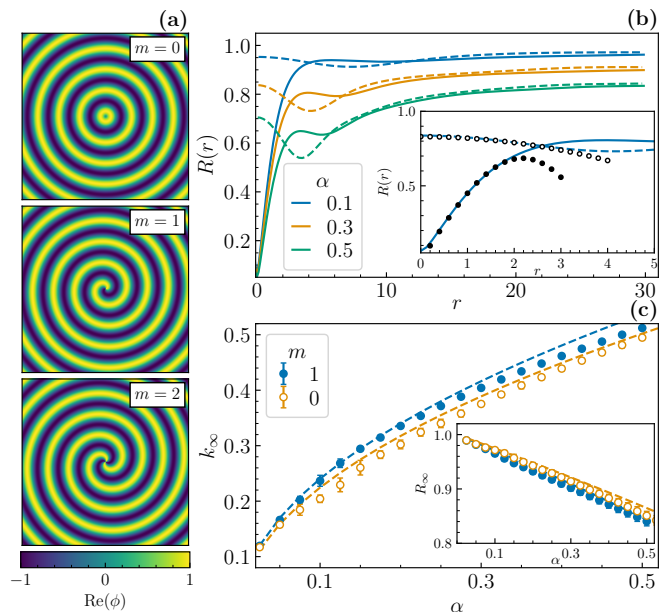


FIG. 2. (a) Defect solutions of the NRCH model for various values of  $m$ . Defects with  $|m| = 0, 1$  are stable. Defects with  $|m| > 1$  are not stable and evolve into bound pairs of  $|m| = 1$  defects. (b)  $R(r)$  vs.  $r$  for  $m = 0$  and  $1$  at different  $\alpha$ . Inset: Comparison of the numerical solutions of  $R(r)$  with small  $r$  approximations [34]. (c) Selected wave number  $k_\infty$  vs.  $\alpha$ . We find  $k_\infty = C\sqrt{\alpha}$  (dashed lines with corresponding colours), with  $C \sim 0.76$  for  $m = 1$  and  $C \sim 0.7$  for  $m = 0$ . Inset:  $R_\infty$  vs.  $\alpha$  (dashed lines show  $\sqrt{1 - k_\infty^2}$ ).

unstable and evolve into a bound pair of unit magnitude spirals [34].

Defects are the generators of plane waves travelling outwards in the radial direction (see Movie 1). Thus, at large distances from the defect core ( $r \gg 1$ ), the wave front approaches a plane wave, i.e.  $k(r) \rightarrow k_\infty$ , and  $R(r) \rightarrow R_\infty = \sqrt{1 - k_\infty^2}$ . The stability of the emanated plane waves implies that defect solutions are also stable at large distances from their core, and they screen the defect core from outside perturbations [36]. In Fig. 2(c), we plot the selected wavenumber  $k_\infty = C\sqrt{\alpha}$  for different values of  $\alpha$ ; the inset verifies the relation between  $R_\infty$  and  $k_\infty$ .  $R_\infty$  vanishes and defect solutions cease to exist for  $\alpha \geq \alpha_\times \equiv C^{-2}$ . Multi-stability of the plane waves for all  $q < 1$  then implies a potential crossover from defects to travelling waves for  $\alpha \geq \alpha_\times$ . The impossibility of defect solutions beyond  $\alpha_\times$  is also clear from the fact that the selected wavenumber is larger than the spinodal instability cutoff ( $k_\infty > 1$ ), and its amplitude will eventually vanish.

*Defect networks in simulations.*—At equilibrium ( $\alpha = 0$ ), a system quenched from a high temperature disordered state to sub-critical temperatures undergoes bulk phase separation. The phase separated domains grow with time and a unique growing length scale characterizes this coarsening dynamics [37, 38]. The dense-

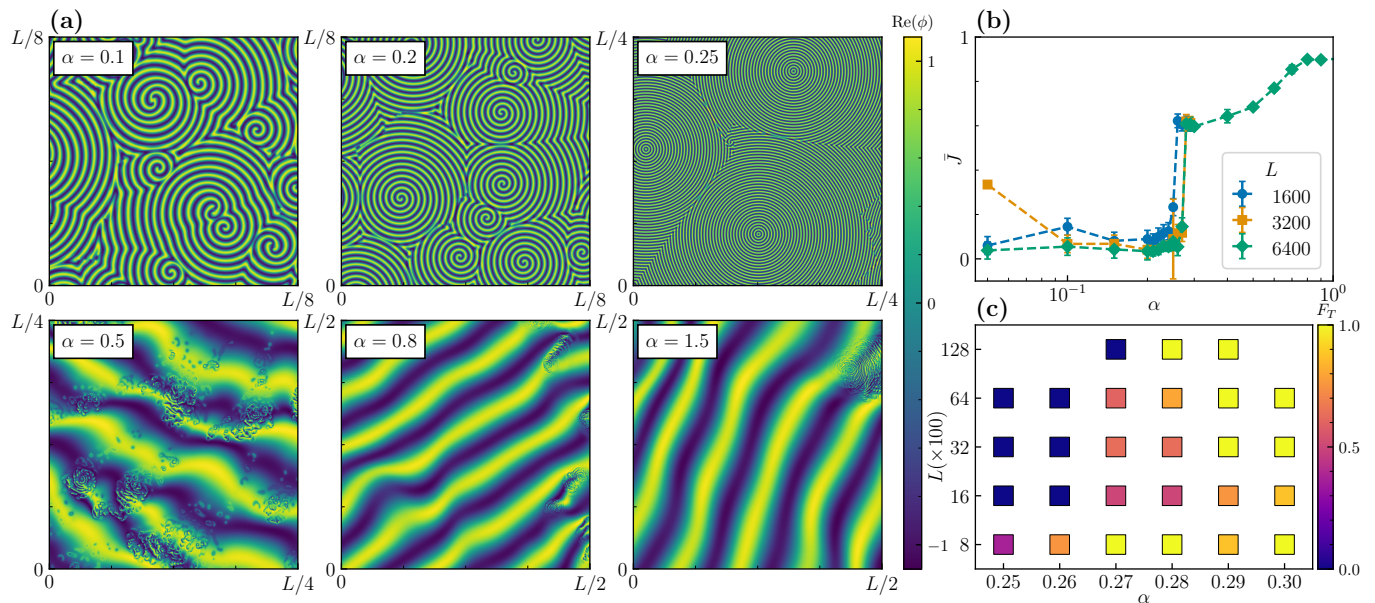


FIG. 3. (a) Transition from disordered defect networks to travelling waves on increasing the non-reciprocity strength  $\alpha$  for system size  $L = 6400$  [34]. We plot the real component of  $\phi$  at long times on smaller subdomains for a better visual representation. (b) Global polar order in the steady state with varying  $\alpha$ . At  $\alpha_c$ , we observe a sharp order-disorder transition. (c) Plot of the fraction of simulations ( $F_T$ ) that transition to travelling waves for different  $\alpha$  and  $L$ . For  $\alpha \geq 0.28$ , almost all of the simulations show the transition and hence we infer  $\alpha_c = 0.28 \pm 0.01$ . Due to the finite size effects, smaller boxes can show transition at slightly smaller values of  $\alpha$  [34].

dense (liquid-liquid) or dense-dilute (liquid-gas) coexistence states are determined by the reciprocal interactions between the two scalar fields. For  $\alpha \neq 0$ , the interplay of non-reciprocity with equilibrium forces allows for the emergence of *a priori* undetermined complex spatio-temporal patterns; a hallmark feature of non-equilibrium systems [10, 39–41]. To understand the dynamical features of the NRCH model, we perform large scale simulations of (1) with varying non-reciprocity  $\alpha$  and system size  $L$  [34]. In Fig. 3(a), we show the typical steady-state solutions obtained from the evolution of a disordered state. A critical threshold of non-reciprocal interactions,  $\alpha_c$ , separates the phase space into two distinct regimes – quasi-stationary defect networks and travelling waves superimposed with local fluctuations [34]. In what follows, we highlight the main features of these non-equilibrium states; a detailed analysis will be presented elsewhere.

For  $\alpha < \alpha_c$  [see Fig. 3(a) (top panels)], after an initial transient period in which numerous newly-born defects waltz around and merge, a frozen steady-state emerges where the defects settle down in a stable quasi-stationary configuration (see Movie 2). At low values of  $\alpha$ , we observe isolated spirals and a few bound pairs of like-charged spirals that orbit around a common centre. As we increase  $\alpha$ , targets emerge as well and are the dominant defects in the network. Right below  $\alpha_c$ , we primarily observe targets. Inter-defect separation increases with  $\alpha$  but does not show a clear trend, although tar-

gets show a strikingly higher inter-defect separation as compared to the spirals. The spatial distribution of the defects is highly dependent on the initial conditions, and we find that a randomly chosen defect configuration respecting typical inter-defect separation and defect density remains stationary. We observe limited dynamics in the defect networks: the arms of the isolated spirals rotate with the frequency  $\omega$ , the targets pulsate, and the spiral cores that form bound pairs orbit around a common centre. Numerous additional defects—at very small separations from each other—are observed at the intersections of defect boundaries. These defects show dynamical rearrangement and form locally unsteady patches in an otherwise stationary network (see Movie 2).

For  $\alpha \gtrsim \alpha_c$ , we find travelling waves [see Fig. 3(a) (bottom panels)]. The transient period shows a mixture of defects and growing patches of polar order, which quickly washes away the defect cores. Afterwards, global polar order, albeit marred by local spatial fluctuations, emerges. These fluctuations decay with time and eventually we find travelling density bands.

To quantify the transition from defect networks to travelling waves we compute the average polar order  $\bar{J} \equiv \left| \left\langle \hat{\mathbf{J}}(\mathbf{r}, t) \right\rangle \right|$ , where  $\mathbf{J}(\mathbf{r}, t) \equiv \frac{1}{2i} (\phi^* \nabla \phi - \phi \nabla \phi^*) = \phi_1 \nabla \phi_2 - \phi_2 \nabla \phi_1$  is the polar order parameter and  $\langle \dots \rangle$  implies averaging over space and time in the steady-state. For a monochromatic plane wave of the form (2),  $\mathbf{J} = R^2 \mathbf{q}$ , and thus  $\bar{J} = 1$ . On the other hand, for

defect solutions (3), we have  $\mathbf{J} = R(r)^2 \left( k(r)\hat{r} + \frac{m}{r}\hat{\theta} \right)$ , which implies  $\bar{J} \sim 0$ . Far away from the defect cores ( $r \gg \ell$ ), we obtain  $\mathbf{J} \sim R_\infty^2 k_\infty \hat{r}$ , which is independent of the value of  $m$ . The defects emanate radially outward travelling waves and  $\mathbf{J}$  has a topological singularity with unit positive charge at the defect core.

As shown in Fig. 3(b), the transition from defect networks to travelling waves is marked by a sharp increase in the average polar order  $\bar{J}$  at  $\alpha = \alpha_c$ , consistently across various box sizes ( $L$ ). We find that  $\bar{J} \sim 0$  for defect networks ( $\alpha < \alpha_c$ ), while it acquires a finite value for the travelling wave states  $\alpha > \alpha_c$ . Spatial fluctuations decrease with increasing  $\alpha$ , thus  $\bar{J} < 1$  for  $\alpha \gtrsim \alpha_c$ , while it saturates close to its maximum permissible value  $\bar{J} = 1$  for  $\alpha \gg \alpha_c$ . We find that the finite size effects could alter the nature of steady states observed for  $\alpha$  close to the critical value  $\alpha_c$ . We have performed numerical simulations with different realizations of initial conditions at varying box sizes ( $L$ ) spanning two orders of magnitude. In Fig. 3(c), the fraction of simulations that reached a travelling wave steady state is shown for various  $L$  and  $\alpha$  values close to the expected  $\alpha_c$ . From these simulations, we infer  $\alpha_c = 0.28 \pm 0.01 \ll \alpha_\times$ .

*Discussion.*—Non-reciprocal interactions emerge naturally in non-equilibrium systems with complex interactions [4, 42], and this effective breaking of the action-reaction symmetry leads to a variety of novel features. Here, we have unveiled a new feature of non-reciprocal interactions, namely, the emergence of topological defects in binary mixtures of conserved scalar densities. We find two kind of defects for the NRCH model, spirals with a unit magnitude topological charge and neutral targets. For a given  $\alpha$ , defects with a unique wavenumber are selected, which immediately predicts a crossover from defects to plain waves at  $\alpha = \alpha_\times$ . However, our large-scale numerical simulations show a disorder-order transition from quasi-stationary defect networks to imperfect global polar order  $\alpha = \alpha_c \ll \alpha_\times$ . These states show a rich phase space behaviour. While both charged and neutral solutions are allowed for any  $\alpha < \alpha_\times$ , at low  $\alpha$  the system prefers to spontaneously break the chiral symmetry and we find isolated and bound pairs of spirals. On the other hand, close to  $\alpha_c$ , targets are the preferred defects. Above  $\alpha_c$ , the noisy travelling waves with spontaneously broken polar symmetry emerge. The fluctuations in these states decay with time, but can persist for a very long duration especially for  $\alpha \gtrsim \alpha_c$ .

Our study uncovers important features concerning on the phenomenology of active matter with non-reciprocal interactions. We note here that while the isolated defect solutions are stable in the presence of persistent noise, wave interaction and finite size effects can result in interesting pattern formation (see Movie 3). A natural next step will be to study the stability of isolated defect solutions to small perturbations, as has been in the case of

the CGL equation [27, 33], for which it has been observed that the defect network states are not static but evolve extremely slowly [43]. It will be interesting to investigate if the defect networks in the NRCH model exhibit the phases of vortex liquid and vortex glass with intermittent slow relaxation observed in CGL. We have focused here on a simplified version of the NRCH model with purely non-reciprocal interactions at the linear level and restored global rotational symmetry in the  $\phi$ -space [34]. In the Supplemental Material [34] we show the defect solutions in the presence of linear reciprocal interactions. In the future, our study could be extended to the study of the properties of these defect solutions and to include nonlinear non-reciprocal interactions [21].

We acknowledge fruitful discussions with Giulia Pisegna and Suropriya Saha, and support from the Max Planck School Matter to Life and the MaxSynBio Consortium which are jointly funded by the Federal Ministry of Education and Research (BMBF) of Germany and the Max Planck Society.

- 
- [1] G. Gompper, R. G. Winkler, T. Speck, A. Solon, C. Nardini, F. Peruani, H. Löwen, R. Golestanian, U. B. Kaupp, L. Alvarez, T. Kiorboe, E. Lauga, W. C. K. Poon, A. DeSimone, S. Muiños-Landin, A. Fischer, N. A. Söker, F. Cichos, R. Kapral, P. Gaspard, M. Ripoll, F. Sagues, A. Doostmohammadi, J. M. Yeomans, I. S. Aranson, C. Bechinger, H. Stark, C. K. Hemelrijk, F. J. Nedelec, T. Sarkar, T. Aryaksama, M. Lacroix, G. Duclos, V. Yashunsky, P. Silberzan, M. Arroyo, and S. Kale, *J. Phys.: Condens. Matter* **32**, 193001 (2020).
  - [2] R. Soto and R. Golestanian, *Phys. Rev. Lett.* **112**, 068301 (2014).
  - [3] S. Saha, S. Ramaswamy, and R. Golestanian, *New Journal of Physics* **21**, 063006 (2019).
  - [4] A. V. Ivlev, J. Bartnick, M. Heinen, C.-R. Du, V. Nosenko, and H. Löwen, *Phys. Rev. X* **5**, 011035 (2015).
  - [5] M. Ballerini, N. Cabibbo, R. Candelier, A. Cavagna, E. Cisbani, I. Giardina, V. Lecomte, A. Orlandi, G. Parisi, A. Procaccini, M. Viale, and V. Zdravkovic, *Proc. Natl. Acad. Sci.* **105**, 1232 (2008).
  - [6] D. Helbing and P. Molnár, *Phys. Rev. E* **51**, 4282 (1995).
  - [7] D. Helbing, I. Farkas, and T. Vicsek, *Nature* **407**, 487 (2000).
  - [8] K. W. Rio, G. C. Dachner, and W. H. Warren, *Proc. R. Soc. B Biol. Sci.* **285**, 20180611 (2018).
  - [9] A. Dinelli, J. O’Byrne, A. Curatolo, Y. Zhao, P. Sollich, and J. Tailleur, *Non-reciprocity across scales in active mixtures* (2022), arxiv.2203.07757.
  - [10] N. Uchida and R. Golestanian, *Phys. Rev. Lett.* **104**, 178103 (2010).
  - [11] M. Fruchart, R. Hanai, P. B. Littlewood, and V. Vitelli, *Nature* **592**, 363 (2021).
  - [12] S. A. M. Loos and S. H. L. Klapp, *New Journal of Physics* **22**, 123051 (2020).
  - [13] S. Osat and R. Golestanian, *Nat. Nanotechnol.* **18**, 79 (2023).

- [14] R. Soto and R. Golestanian, *Phys. Rev. E* **91**, 052304 (2015).
- [15] J. A. Cohen and R. Golestanian, *Phys. Rev. Lett.* **112**, 068302 (2014).
- [16] J. Agudo-Canalejo and R. Golestanian, *Phys. Rev. Lett.* **123**, 018101 (2019).
- [17] L. P. Dadhichi, J. Kethapelli, R. Chajwa, S. Ramaswamy, and A. Maitra, *Phys. Rev. E* **101**, 052601 (2020).
- [18] R. K. Gupta, R. Kant, H. Soni, A. K. Sood, and S. Ramaswamy, *Phys. Rev. E* **105**, 064602 (2022).
- [19] S. De Karmakar and R. Ganesh, *Phys. Rev. E* **106**, 044607 (2022).
- [20] M. Knežević, T. Welker, and H. Stark, *Scientific Reports* **12**, 10.1038/s41598-022-23597-9 (2022).
- [21] S. Saha, J. Agudo-Canalejo, and R. Golestanian, *Phys. Rev. X* **10**, 041009 (2020).
- [22] Z. You, A. Baskaran, and M. C. Marchetti, *PNAS* **117**, 19767 (2020).
- [23] S. Saha and R. Golestanian, Effervescent waves in a binary mixture with non-reciprocal couplings (2022), arXiv:2208.14985.
- [24] T. Frohoff-Hülsmann, J. Wrembel, and U. Thiele, *Phys. Rev. E* **103**, 042602 (2021).
- [25] T. Frohoff-Hülsmann and U. Thiele, *IMA J. Appl. Math.* **86**, 924 (2021).
- [26] T. Frohoff-Hülsmann and U. Thiele, Nonreciprocal Cahn-Hilliard equations emerging as one of eight universal amplitude equations (2023), arXiv:2301.05568.
- [27] P. S. Hagan, *SIAM J. Appl. Math.* **42**, 762 (1982).
- [28] A. N. Zaikin and A. M. Zhabotinsky, *Nature* **225**, 535 (1970).
- [29] A. T. Winfree, *Science* **175**, 634 (1972).
- [30] Y. Kuramoto, *Chemical Oscillations, Waves, and Turbulence*, edited by H. Haken, Springer Series in Synergetics, Vol. 19 (Springer Berlin Heidelberg, Berlin, Heidelberg, 1984).
- [31] K. J. Lee, E. C. Cox, and R. E. Goldstein, *Phys. Rev. Lett.* **76**, 1174 (1996).
- [32] M. Hendrey, K. Nam, P. Guzdar, and E. Ott, *Phys. Rev. E* **62**, 7627 (2000).
- [33] I. S. Aranson and L. Kramer, *Rev. Mod. Phys.* **74**, 99 (2002).
- [34] Supplemental Material available at ????. It includes a description of the movies, a discussion on the NRCH model and its various solutions, numerical methods and finite-size effects on the defect solutions, and Ref. [44].
- [35] W. Zimmermann, *Physica A: Statistical Mechanics and its Applications* **237**, 405 (1997).
- [36] I. S. Aranson, L. Kramer, and A. Weber, *Phys. Rev. E* **47**, 3231 (1993).
- [37] A. J. Bray, *Advances in Physics* **51**, 481 (2002).
- [38] A. Onuki, *Phase Transition Dynamics* (Cambridge University Press, Cambridge; New York, 2002).
- [39] M. C. Cross and P. C. Hohenberg, *Rev. Mod. Phys.* **65**, 851 (1993).
- [40] M. C. Marchetti, J. F. Joanny, S. Ramaswamy, T. B. Liverpool, J. Prost, M. Rao, and R. A. Simha, *Rev. Mod. Phys.* **85**, 1143 (2013).
- [41] S. Ramaswamy, *Annu. Rev. Condens. Matter Phys.* **1**, 323 (2010).
- [42] R. Golestanian, in *Active matter and nonequilibrium statistical physics*, Lecture Notes of the 2018 Les Houches Summer School (Oxford University Press, London, England, 2022).
- [43] C. Brito, I. S. Aranson, and H. Chaté, *Phys. Rev. Lett.* **90**, 068301 (2003).
- [44] S. Cox and P. Matthews, *Journal of Computational Physics* **176**, 430 (2002).